Title: Insight into motility-dependent pathogenicity of the zoonotic spirochete *Leptospira*

Short title: Motility-dependent spirochetal pathogenicity

Authors: Jun Xu[1*], Nobuo Koizumi[2], Shuichi Nakamura[3]

Affiliations:

[1]Department of Animal Microbiology, Graduate School of Agricultural Science, Tohoku University, Sendai, Miyagi, Japan

[2]Department of Bacteriology I, National Institute of Infectious Diseases, Shinjuku-ku, Tokyo, Japan

[3]Department of Applied Physics, Graduate School of Engineering, Tohoku University, Sendai, Miyagi, Japan

Corresponding author: Shuichi Nakamura, Department of Applied Physics, Graduate School of Engineering, Tohoku University, 6-6-05 Aoba, Aoba-ku, Sendai, Miyagi 980-8579, Japan.

Contact: naka@bp.apph.tohoku.ac.jp

***Present address:** Department of Bacteriology, Graduate School of Medicine, University of the Ryukyus

Abstract

Bacterial motility is crucial for many pathogenic species in the process of invasion and/or dissemination. The spirochete bacteria *Leptospira* spp. cause symptoms, such as hemorrhage, jaundice, and nephritis, in diverse mammals including humans. Although loss-of-motility attenuate the spirochete, the mechanism of the motility-dependent pathogenicity is unknown. Here, focusing on that *Leptospira* spp. swim in liquid and crawl on solid surfaces, we investigated the spirochetal dynamics on the host tissues by infecting cultured kidney cells from various species with pathogenic and nonpathogenic leptospires. We found that, in the case of the pathogenic leptospires, a larger fraction of bacteria attached to the host cells and persistently traveled long distances using the crawling mechanism. Our results associate the kinetics and kinematic features of the spirochetal pathogens with their virulence.

One Sentence Summary: Adhesivity and crawling motility over host tissue surfaces are closely related to the pathogenicity of a zoonotic spirochete.

Introduction

Many bacteria utilize motility to explore environments for survival and prosperity. For pathogenic species, the motility is a virulence factor, harming the host animal or plant health(*6*). For example, *Helicobacter pylori* requires motility to migrate towards the epithelial tissue in the stomach(*7*), and motility and chemotaxis are key factors that guide host invasion in different *Salmonella* serovars (*8, 9*). Movement and adhesion of the Lyme disease spirochete *Borrelia burgdorferi* in blood vessels are thought to be important during the process of host cell invasion(*10*). In the enteric pathogens, such as the enteropathogenic *Escherichia coli* (EPEC), the motility

machinery flagella are also important for adhesion to the host intestinal epithelium(*11*).

In this study, we address the association of bacterial motility with pathogenicity in the worldwide zoonosis leptospirosis. The causative agent of leptospirosis *Leptospira* spp. are Gram-negative bacteria belonging to the phylum Spirochaetes. The genus *Leptospira* is comprised of pathogenic, intermediate, and nonpathogenic species, which are classified into over 300 serovars defined based on the structural diversity of lipopolysaccharide (LPS)(*2, 12*). The pathogenic species affect various mammalian hosts such as livestock (cattle, pigs, horses, and others), companion animals (dogs and others), and humans, causing severe symptoms, such as hemorrhage, jaundice, and nephritis in some host-serovar pairs(*2–4*). The leptospires can be maintained in the renal tubules of recovered animals or reservoir hosts, and the urinary shedding of leptospires to the environment leads to infection in humans and other animals through contact with contaminated soil or water. Although the pathogenic mechanism of leptospirosis is not well elucidated, in addition to the pathogen-specific proteins such as Loa22(*13*), their motility using two periplasmic flagella (PFs) beneath the outer cell membrane (Fig. 1A) is known to be somehow involved in the infection and pathogenicity based on studies in animal models that have shown attenuation of the spirochetes by loss-of-motility(*14, 15*).

The rotation of the PFs in *Leptospira* gyrates both ends of the cell body and rotates the coiled cell body, allowing the spirochete not only to swim in fluids but also to crawl over solid surfaces(*16, 17*). Adherence and entry of pathogenic leptospires in the conjunctival epithelium(*4*) and in the paracellular routes of hepatocytes(*18*) were previously observed using scanning electron microscopy, suggesting adhesion to the host tissue surfaces and subsequent crawling of pathogenic leptospires. To verify this hypothesis, assuming the transition of leptospires between swimming and adhesion states

and between adhesion and crawling states in the equilibrium (Fig. 1B), we investigated the adhesion and crawling motility of *Leptospira* on the cultured kidney cells of various mammalian species.

Results

Steady-state analysis of *Leptospira* on the kidney cells. We infected cultured kidney cells from six different host species (rat, dog, monkey, mouse, cow, and human) with three *Leptospira* strains (the pathogenic *L. interrogans* serovars Icterohaemorrhagiae and Manilae, and the nonpathogenic *L. biflexa* serovar Patoc) expressing green fluorescent protein (GFP) within a chamber slide (Fig. 2A). We observed the *Leptospira* cells by epi-fluorescent microscopy (Fig. 2B) and measured the fractions of swimming [S], adhered [A], and crawling [C] bacteria on the kidney cells (Fig. 2C). Figs. 2D-E show that almost half of the pathogenic population transited from the swimming state to the adhesion and crawling states, whereas >75% non-pathogenic leptospires remained in the swimming state. We calculated the equilibrium constant between swimming and adhesion states ($K_{S\text{-}A}$) and between adhesion and crawling states ($K_{A\text{-}C}$) from the cell fractions using $K_{S\text{-}A} = [A] / [S]$ and $K_{A\text{-}C} = [C] / [A]$, respectively. The pathogenic leptospires had a significantly larger $K_{A\text{-}C}$ in comparison with the nonpathogenic strain ($P < 0.05$); $K_{S\text{-}A}$ did not seem to correlate to virulence (Fig. 2F). These thermodynamic parameters suggest that the biased transition from adhesion to crawling would be responsible for the virulence of *Leptospira* (Fig. 2G).

Crawling motility. Taking the results of the steady-state analysis, we focused on the crawling motility of individual *Leptospira* cells on the kidney cells. Although the crawling speed varied among the measured host-bacterium pairs, *L. interrogans* serovar Icterohaemorrhagiae showed

significantly faster speed than the others, indicating the species/serovar dependence of the crawling ability (Fig. 3A). On the other hand, there is no difference in crawling speed between *L. interrogans* serovar Manilae and *L. biflexa* serovar Patoc, suggesting that the crawling speed itself is not related to leptospiral virulence. Meanwhile, we observed that some leptospiral cells attached to the kidney cells and moved smoothly for periods, migrating over long-distances (upper panels of Figs. 3B-C; Movie S2), whereas others frequently reversed the crawling direction (lower panels of Figs. 3B-C; Movie S3). Cell movements with reversals are considered to be diffusive and thus can be evaluated by plotting the mean square displacement (MSD) against time, a general methodology for diffusion (Brownian motion) analysis(*19*). The MSD of simple diffusion without directivity is proportional to time, and therefore double-logarithmic MSD plots from such non-directional diffusion represent slopes of ~1, whereas those from directive movements show MSD slopes of ~2, representing the relatively long distance traveled by the cells (Fig. S1). Double-logarithmic MSD plots obtained from each individual leptospires showed a wide range of MSD slopes (example data are shown in Fig. 3D) and differed for each host-*Leptospira* pair (Fig. 3E left and Fig. S2). The nonpathogenic strain showed the slope of ~1, while the pathogenic strains had significantly larger slopes that denote directive motion (Fig. 3E right). Thus, concerning the crawling motility, directivity and persistency rather than speed could be crucial for virulence.

Discussion

Our results suggested the importance of adhesion to and persistent crawling on the host tissue for the pathogenicity of *Leptospira*. The thermodynamic and kinematic parameters are associated in Fig 4A, showing the tendency that pathogenic species are biased to the crawling state and can migrate longer

105 distance on the host tissue surfaces. The crawling motility of *Leptospira* is caused by the attachment
106 of the spirochete cell body to surfaces via adhesive cell surface components(*16, 20*). The successive
107 alternation in the attachment and detachment of adhesins allows for this progressive movement by
108 the spirochetes, however, an excessively strong adhesion can inhibit crawling(*16*). LPS, the
109 molecular basis for the identification of the different *Leptospira* serovars(*2, 12*), is thought to be a
110 crucial adhesin important for this crawling motion(*16*). Thus, it is possible that compatibility of the
111 serological characteristics of leptospires and the surface properties of the host tissue might affect the
112 crawling behavior over the tissue surfaces and the subsequent clinical consequences. The results of
113 our biophysical experiments outline a plausible framework for the adhesion and crawling-dependent
114 pathogenicity of *Leptospira* (Fig. 4B). The biased transition from the adhesion to the crawling state
115 and the long-distance, persistent crawling allows leptospires to explore the host's cell surfaces,
116 increasing the probability of encountering routes for invasion through their intracellular tight
117 junctions (Fig. 4B, left). In contrast, the swimming or weakly attached leptospires can be swept by
118 external forces, such as intermittent urination, and diffusive crawling by which leptospires cannot be
119 disseminated over host tissues will not be involved in invasion (Fig. 4B, right).

120 Some bacterial pathogens are specialized to invade a very limited array of hosts, whereas others
121 can infect multiple host species. The host range differs for each pathogen and the clinical symptoms
122 depend on each host-pathogen combination. The same applies for leptospirosis, the outcome of
123 *Leptospira* infection depends on the host-serovar association, and some animal species can become
124 an asymptomatic reservoir for particular *Leptospira* serovars. The present experiments also provided
125 data allowing us to discuss the host dependence of the leptospiral dynamics. Among the investigated
126 materials, serovar Manilae vs rats and serovar Icterohaemorrhagiae vs rats are typically

asymptomatic pairs, and Fig. 4A shows that the pairs with reservoirs have lower scores in comparison with those causing severe symptoms, such as Manilae vs humans, Icterohaemorrhagiae vs dogs, and others. This implies that the surface dynamics of the spirochete could be related to their host-dependent pathogenicity. Understanding the mechanism of the host preferences by pathogens is important for prevention of the infection spread, but the host-pathogen association in leptospirosis is ambiguous. Also, microarray analyses have revealed that regulation of gene expression in *Leptospira* is affected by its interaction with host cells(*21*, *22*). Although host immune responses against *Leptospira* infection remain mostly unknown, pathogenic leptospires interfere with the complement system through the degradation of complement proteins(*23*) and inhibition of coagulation via binding to thrombin(*24*). Thus, abundant factors in both bacteria and hosts should be investigated for a deeper understanding of the host-dependent pathogenicity.

Materials and Methods

***Leptospira* strains and growth conditions.** Pathogenic serovars of *L. interrogans* serovar Icterohaemorrhagiae (strain WFA135), an isolate from *Rattus norvegicus* in Tokyo, Japan, serovar Manilae (strain UP-MMC-NIID)(*25*, *26*) and a saprophytic *L. biflexa* serovar Patoc (strain Patoc I) were used in this study. The serovar of WFA135 was determined by multiple loci variable number of tandem repeats analysis (MLVA) and DNA sequencing of the *lic12008* gene(*26*, *27*). Bacteria were cultured in enriched Ellinghausen-McCullough-Johnson-Harris (EMJH) liquid medium (BD Difco, NJ, USA) containing 25 μg/mL spectinomycin at 30 °C for 2 (*L. biflexa*) or 4 (*L. interrogans*) days until the stationary phase. To track *Leptospira* cells when in co-culture with mammalian kidney cells, a green fluorescent protein (GFP) was constitutively expressed in each strain (Fig. 1D; Movie S1).

Mammalian cells and media. Mammalian kidney epithelial cell lines used included MDCK-NBL2 (dog), NRK-52E (rat), Vero (monkey), MDBK-NBL1 (cow), TCMK-1 (mouse), and HK-2 (human). MDCK, Vero, TCMK, and MDBK cells were maintained in Eagle's minimum essential media (MEM) (Sigma-Aldrich, Darmstadt, Germany) containing 10% fetal bovine serum or 10% horse serum (Nacalai Tesque, Kyoto, Japan) at 37 °C and 5% CO_2. NRK cells were maintained in Dulbecco's modified Eagle's media (DMEM) (Thermo Fisher Scientific, MA, USA) with 4 mM L-glutamine, adjusted to contain 1.5 g/L sodium bicarbonate and 4.5 g/L glucose, and with 5% bovine calf serum (Nacalai Tesque) at 37 °C and 5% CO_2. HK-2 cells were maintained in keratinocyte serum-free (KSF) media with 0.05 mg/mL bovine pituitary extract and 5 ng/mL human recombinant epidermal growth factor (Gibco - Thermo Fisher Scientific, MA, USA). All culture conditions contained a 5% antibiotic / antimycotic mixed solution (Nacalai Tesque). Cells were treated with a 0.1% trypsin - EDTA solution (Nacalai Tesque) to dislodge the cells during each passage process.

GFP expression in *L. interrogans* and *L. biflexa.* For the construction of a replicable plasmid in *L. interrogans*, the corresponding *rep-parB-parA* region of the plasmid pGui1 from the *L. interrogans* serovar Canicola strain Gui44 plasmid pGui1(*28*) was amplified from a *L. interrogans* serogroup Canicola isolate, and the amplified product was cloned into the PCR-generated pCjSpLe94(*29*) by NEBuilder HiFi DNA Assembly cloning (New England BioLabs), generating pNKLiG1. The *flgC* promoter region and *gfp* were amplified from pCjSpLe94 and pAcGFP1 (Clontech), respectively, and the amplified products were cloned into the *Sal*I-digested pNKLiG1 for *L. interrogans* or the

171 *Sal*I-digested pCjSpLe94 for *L. biflexa*. The plasmids were transformed into strains WFA135,
172 UP-MMC-NIID or Patoc I by conjugation with *E. coli* β2163 harboring the plasmid(*30*). Primer
173 sequences used in this study are listed in Table S1. Expression of GFP did not affect motility in the
174 *Leptospira* serovars (Fig. S3).
175
176 **Preparation of kidney cells and *Leptospira* cells in a chamber slide.** Kidney cells were harvested
177 with 0.1% trypsin and 0.02% EDTA in a balanced salt solution (Nacalai Tesque) and plated onto a
178 chamber slide (Iwaki, Tokyo, Japan) using their corresponding media without antibiotics. The slides
179 were incubated for 48 h until a monolayer was formed and washed twice with media to remove
180 non-adherent cells. The cells were incubated for a further 2 h at 37 °C and 5% CO_2. Approximately
181 500 ml of stationary phase *Leptospira* cells were harvested by centrifugation at 1,000 *g* for 10 min at
182 room temperature, washed twice in PBS, then resuspended in the corresponding kidney cell culture
183 media without antibiotics at 37 °C to a concentration of 10^7 cells / ml. These suspensions (1 ml) were
184 then added into the corresponding chamber slides containing the kidney cell layer, and the chamber
185 slides were incubated at 37 °C for 1 h.
186
187 **Microscopy observation and adhesion-crawling assay.** The movement behaviors, swimming,
188 adhesion and crawling of the *Leptospira* cells on the kidney cells were observed using a dark-field
189 microscope (BX53, Splan 40×, NA 0.75, Olympus, Tokyo, Japan) with an epi-fluorescent system
190 (U-FBNA narrow filter, Olympus) and recorded by a CCD-camera (WAT- 910HX, Watec Co.,
191 Yamagata, Japan) at 30 frames per second. *Leptospira* cells were tracked using an ImageJ (NIH, MD,
192 USA)-based tracking system and the motion parameters such as motile fraction, velocity and MSD

were analyzed using Excel-based VBA (Microsoft, WA, USA). The two-dimensional MSD of individual leptospiral cells during a period Δt was calculated by the following equation: $MSD(\Delta t) = \langle (x_{i+\Delta t} - x_i)^2 + (y_{i+\Delta t} - y)^2 \rangle$, where ($x_i$, y_i) is the bacterial position at I (see also Supplementary Fig. 1).

Statistical analysis. All experiments were performed in triplicate. Statistical differences between data were evaluated using a Student's *t*-test. The data clustering was performed independently for each experiment using the k-means method in OriginPro (OriginLab Corp., MA, USA). The clustering method grouped the data population into a specified number of clusters referring to the Euclidian distance of each data point from the centroid of the cluster, calculated at every clustering process, and reclassifying the data point to the nearest cluster.

Supplementary Materials

Tables S1. Primer sequences used in this study

Fig. S1. Explanation of MSD plot.

Fig. S2. Histograms of the MSD slopes

Fig. S3. Effect of GFP expression on the *Leptospira* motility.

Movie S1. Epi-fluorescent images of *L. interrogans* on the rat kidney cell

Movie S2. Progressive, long-distance crawling of *L. interrogans* on the monkey kidney cells

Movie S3. Crawling of *L. interrogans* with highly frequent reversal on the dog kidney cells

References

1. A. Bäumler, F. C. Fang, Host specificity of bacterial pathogens. *Cold Spring Harb. Perspect. Med.* **3** (2013), doi:10.1101/cshperspect.a010041.

2. M. Picardeau, Virulence of the zoonotic agent of leptospirosis: still terra incognita? *Nat. Rev. Microbiol.* **15**, 297–307 (2017).

3. B. Adler, A. de la Peña Moctezuma, *Leptospira* and leptospirosis. *Vet. Microbiol.* **140**, 287–296 (2010).

4. A. R. Bharti, J. E. Nally, J. N. Ricaldi, M. A. Matthias, M. M. Diaz, M. A. Lovett, P. N. Levett, R. H. Gilman, M. R. Willig, E. Gotuzzo, J. M. Vinetz, Peru-United States Leptospirosis Consortium, Leptospirosis: a zoonotic disease of global importance. *Lancet Infect. Dis.* **3**, 757–771 (2003).

5. P. N. Levett, Leptospirosis. *Clin. Microbiol. Rev.* **14**, 296–326 (2001).

6. C. Josenhans, S. Suerbaum, The role of motility as a virulence factor in bacteria. *Int. J. Med. Microbiol.* **291**, 605–614 (2002).

7. M. Clyne, T. Ocroinin, S. Suerbaum, C. Josenhans, B. Drumm, Adherence of isogenic flagellum-negative mutants of *Helicobacter pylori* and *Helicobacter mustelae* to human and ferret gastric epithelial cells. *Infect. Immun.* **68**, 4335–4339 (2000).

8. J. E. Olsen, K. H. Hoegh-Andersen, J. Casadesús, J. T. Rosenkrantz, M. S. Chadfield, L. E. Thomsen, The role of flagella and chemotaxis genes in host pathogen interaction of the host adapted *Salmonella enterica* serovar Dublin compared to the broad host range serovar *S.*Typhimurium. *BMC Microbiol.* **13**, 67 (2013).

9. A. Siitonen, M. Nurminen, Bacterial motility is a colonization factor in experimental urinary tract infection. *Infect. Immun.* **60**, 3918–3920 (1992).

10. R. Ebady, A. F. Niddam, A. E. Boczula, Y. R. Kim, N. Gupta, T. T. Tang, T. Odisho, H. Zhi, C. A. Simmons, J. T. Skare, T. J. Moriarty, Biomechanics of *Borrelia burgdorferi* vascular interactions. *Cell Rep.* **16**, 2593–2604 (2016).

11. C. P. Cheney, P. A. Schad, S. B. Formal, E. C. Boedeker, Species specificity of *in vitro Escherichia coli* adherence to host intestinal cell membranes and its correlation with *in vivo* colonization and infectivity. *Infect. Immun.* **28**, 1019–1027 (1980).

12. G. M. Cerqueira, M. Picardeau, A century of *Leptospira* strain typing. *Infect. Genet. Evol. J. Mol. Epidemiol. Evol. Genet. Infect. Dis.* **9**, 760–768 (2009).

13. P. Ristow, P. Bourhy, F. W. da Cruz McBride, C. P. Figueira, M. Huerre, P. Ave, I. S. Girons, A. I. Ko, M. Picardeau, The OmpA-like protein Loa22 is essential for leptospiral virulence. *PLoS Pathog.* **3**, e97 (2007).

14. A. Lambert, M. Picardeau, D. A. Haake, R. W. Sermswan, A. Srikram, B. Adler, G. A. Murray, FlaA proteins in *Leptospira interrogans* are essential for motility and virulence but are not required for formation of the flagellum sheath. *Infect. Immun.* **80**, 2019–2025 (2012).

15. E. A. Wunder, C. P. Figueira, N. Benaroudj, B. Hu, B. A. Tong, F. Trajtenberg, J. Liu, M. G. Reis, N. W. Charon, A. Buschiazzo, M. Picardeau, A. I. Ko, A novel flagellar sheath protein, FcpA, determines filament coiling, translational motility and virulence for the *Leptospira* spirochete. *Mol. Microbiol.* **101**, 457–470 (2016).

16. H. Tahara, K. Takabe, Y. Sasaki, K. Kasuga, A. Kawamoto, N. Koizumi, S. Nakamura, The mechanism of two-phase motility in the spirochete *Leptospira*: Swimming and crawling. *Sci. Adv.* **4**, eaar7975 (2018).

17. P. J. Cox, G. I. Twigg, Leptospiral motility. *Nature*. **250**, 260–261 (1974).

18. S. Miyahara, M. Saito, T. Kanemaru, S. Y. A. M. Villanueva, N. G. Gloriani, S. Yoshida, Destruction of the hepatocyte junction by intercellular invasion of *Leptospira* causes jaundice in a hamster model of Weil's disease. *Int. J. Exp. Pathol.* **95**, 271–281 (2014).

19. A. Kusumi, Y. Sako, M. Yamamoto, Confined lateral diffusion of membrane receptors as studied by single particle tracking (nanovid microscopy). Effects of calcium-induced differentiation in cultured epithelial cells.

Biophys. J. **65**, 2021–2040 (1993).

20. N. W. Charon, C. W. Lawrence, S. O'Brien, Movement of antibody-coated latex beads attached to the spirochete *Leptospira interrogans*. *Proc. Natl. Acad. Sci. U. S. A.* **78**, 7166–7170 (1981).

21. K. Satou, M. Shimoji, H. Tamotsu, A. Juan, N. Ashimine, M. Shinzato, C. Toma, T. Nohara, A. Shiroma, K. Nakano, K. Teruya, Y. Terabayashi, S. Ohki, N. Koizumi, S. Okano, T. Suzuki, T. Hirano, Complete genome sequences of low-passage virulent and high-passage avirulent variants of pathogenic *Leptospira interrogans* serovar Manilae strain UP-MMC-NIID, originally isolated from a patient with severe leptospirosis, determined using PacBio single-molecule real-time technology. *Genome Announc.* **3** (2015), doi:10.1128/genomeA.00882-15.

22. C. Toma, G. L. Murray, T. Nohara, M. Mizuyama, N. Koizumi, B. Adler, T. Suzuki, Leptospiral outer membrane protein LMB216 is involved in enhancement of phagocytic uptake by macrophages. *Cell. Microbiol.* **16**, 1366–1377 (2014).

23. T. R. Fraga, D. D. S. Courrol, M. M. Castiblanco-Valencia, I. Y. Hirata, S. A. Vasconcellos, L. Juliano, A. S. Barbosa, L. Isaac, Immune evasion by pathogenic *Leptospira* strains: the secretion of proteases that directly cleave complement proteins. *J. Infect. Dis.* **209**, 876–886 (2014).

24. L. G. Fernandes, Z. M. de Morais, S. A. Vasconcellos, A. L. T. O. Nascimento, *Leptospira interrogans* reduces fibrin clot formation by modulating human thrombin activity via exosite I. *Pathog. Dis.* **73** (2015), doi:10.1093/femspd/ftv001.

25. N. Koizumi, H. Watanabe, Leptospiral immunoglobulin-like proteins elicit protective immunity. *Vaccine*. **22**, 1545–1552 (2004).

26. L. A. Santos, H. Adhikarla, X. Yan, Z. Wang, D. E. Fouts, J. M. Vinetz, L. C. J. Alcantara, R. A. Hartskeerl, M. G. A. Goris, M. Picardeau, M. G. Reis, J. P. Townsend, H. Zhao, A. I. Ko, E. A. Wunder, Genomic

281 comparison among global isolates of *L. interrogans* serovars Copenhageni and Icterohaemorrhagiae
282 identified natural genetic variation caused by an Indel. *Front. Cell. Infect. Microbiol.* **8**, 193 (2018).
283 27. N. Koizumi, H. Izumiya, J.-J. Mu, Z. Arent, S. Okano, C. Nakajima, Y. Suzuki, M. Mizutani Muto, T.
284 Tanikawa, K. R. Taylor, N. Komatsu, K. Yoshimatsu, H. Thi Thu Ha, M. Ohnishi, Multiple-locus
285 variable-number tandem repeat analysis of *Leptospira interrogans* and *Leptospira borgpetersenii* isolated
286 from small feral and wild mammals in East Asia. *Infect. Genet. Evol. J. Mol. Epidemiol. Evol. Genet. Infect.*
287 *Dis.* **36**, 434–440 (2015).
288 28. W.-N. Zhu, L.-L. Huang, L.-B. Zeng, X.-R. Zhuang, C.-Y. Chen, Y.-Z. Wang, J.-H. Qin, Y.-Z. Zhu, X.-K. Guo,
289 Isolation and characterization of two novel plasmids from pathogenic *Leptospira interrogans* serogroup
290 Canicola serovar Canicola strain Gui44. *PLoS Negl. Trop. Dis.* **8**, e3103 (2014).
291 29. M. Picardeau, Conjugative transfer between *Escherichia coli* and *Leptospira* spp. as a new genetic tool. *Appl.*
292 *Environ. Microbiol.* **74**, 319–322 (2008).
293 30. L. Slamti, M. Picardeau, Construction of a library of random mutants in the spirochete *Leptospira biflexa*
294 using a *mariner* transposon. *Methods Mol. Biol. Clifton NJ.* **859**, 169–176 (2012).

295

296 **Acknowledgments** We thank Dr. H. Nishimura (Sendai Medical Center) and Dr. C. Toma
297 (University of the Ryukyus) for the generous gift of animal cell lines; and Dr. E. Isogai (Tohoku
298 University) and Dr. H. Yoneyama (Tohoku University) for the experiment reagents and the insightful
299 discussion. This work was supported by the JSPS KAKENHI: 18K07100 for SN and 18J10834 for
300 JX.

301

302 **Author contributions** J.X., N.K. and S.N. planned the project; J.X and N.K. carried out the

303 experiments; S.N. set up the optical system and programs for data analysis; J.X. and S.N. analyzed
304 the data; J.X., N.K. and S.N. wrote the paper.
305
306 **Competing interests** The authors declare that they have no competing interests.
307
308 **Materials & Correspondence** Shuichi Nakamura; Department of Applied Physics, Graduate School
309 of Engineering, Tohoku University, 6-6-05 Aoba, Aoba-ku, Sendai, Miyagi 980-8579, Japan;
310 naka@bp.apph.tohoku.ac.jp
311
312 **Data availability** The data supporting the findings of this study are available from the corresponding
313 author upon request.

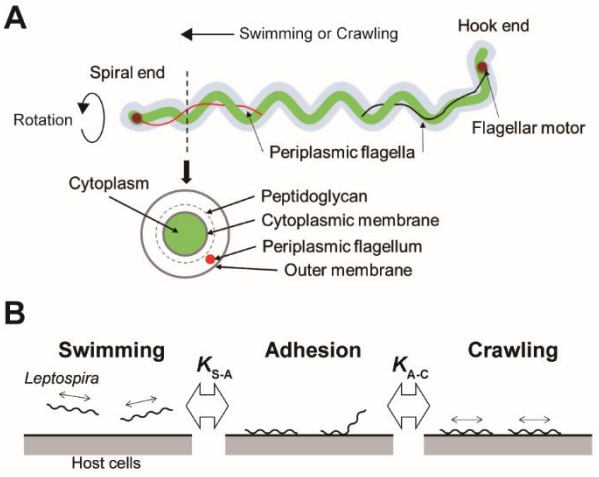

Fig. 1. Structure of *Leptospira* and working model. (A) Schematic diagram of the *Leptospira* cell structure. (B) A three-state kinetic model assuming a transition between "swimming" (floating above cell layers without physical contact to the cells) and "adhesion" (attachment to the cell layer without migration), and between "adhesion" and "crawling" (attachment to the cell layer and movement over surfaces), with K_{S-A} and K_{A-C} represent the equilibrium constants of each transition, respectively.

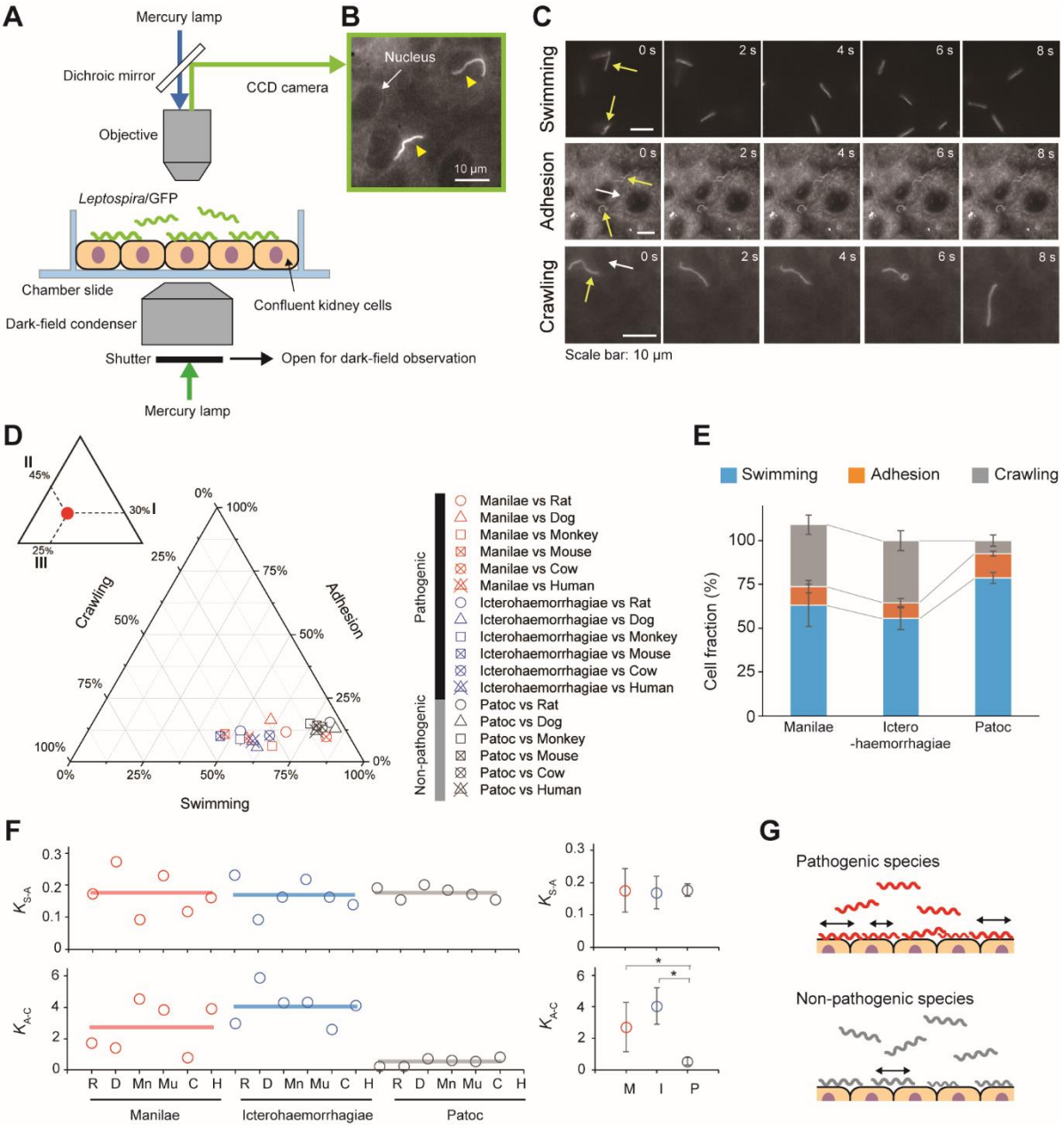

Fig. 2. Steady-state motility and adhesion of *Leptospira* cells on kidney cells. (A) Schematic of the motility assay on the cultured kidney cells by epi-fluorescent microscopy. Fully confluent kidney cells from either animals or humans were cultured in an observation chamber, and *Leptospira* cells that constitutively expressed GFP were added to the cultures. (B) Example of an epi-fluorescence image of the *L. interrogans* serovar Icterohaemorrhagiae, as indicated by the yellow triangles, on the rat kidney cell line, NRK-52E. The nucleus of the kidney cell is shown by the white arrow (Movie S1). (C) Image sequences of swimming (top), adhered (middle), and crawling (bottom) leptospiral

329 cells. Yellow and white arrows indicate *Leptospira* cells and kidney cells, respectively. No kidney
330 cells were observed due to out of focus during the measurement of *Leptospira* cells swimming in
331 liquid media. (D) Ternary plot of the cell fractions in a state of swimming, adhesion, or crawling. The
332 inset schematically explains how to read the ternary plot using an example plot with 30% for I, 45%
333 for II, and 25% for III. Legend is shown to the right of the ternary plot, and M, I and P indicate the *L.*
334 *interrogans* serovar Manilae, *L. interrogans* serovar Icterohaemorrhagiae, and *L. biflexa* serovar
335 Patoc, respectively. Each data point represents the mean of triplicate experiments and ~ 2,400
336 leptospiral cells were measured per host-serovar pair. (E) Average values of the cell fractions. Error
337 bars are the standard deviation. (F) The host-bacterium dependence of the equilibrium constants $K_{S\text{-}A}$
338 and $K_{A\text{-}C}$, calculated from the data shown in **D**; rat (R), dog (D), monkey (Mn), mouse (Mu), cow (C),
339 and human (H). The averaged values determined for each bacterial strain are shown by horizontal
340 lines and are plotted with the standard deviation in the right; *L. interrogans* Manilae (M), *L.*
341 *interrogans* Icterohaemorrhagiae (I), and *L. biflexa* Patoc I (P). The statistical analysis was
342 performed by Mann-Whitney U test (* $P < 0.05$). (G) Schematic explanation of the kinetic difference
343 between pathogenic and non-pathogenic leptospires.
344
345

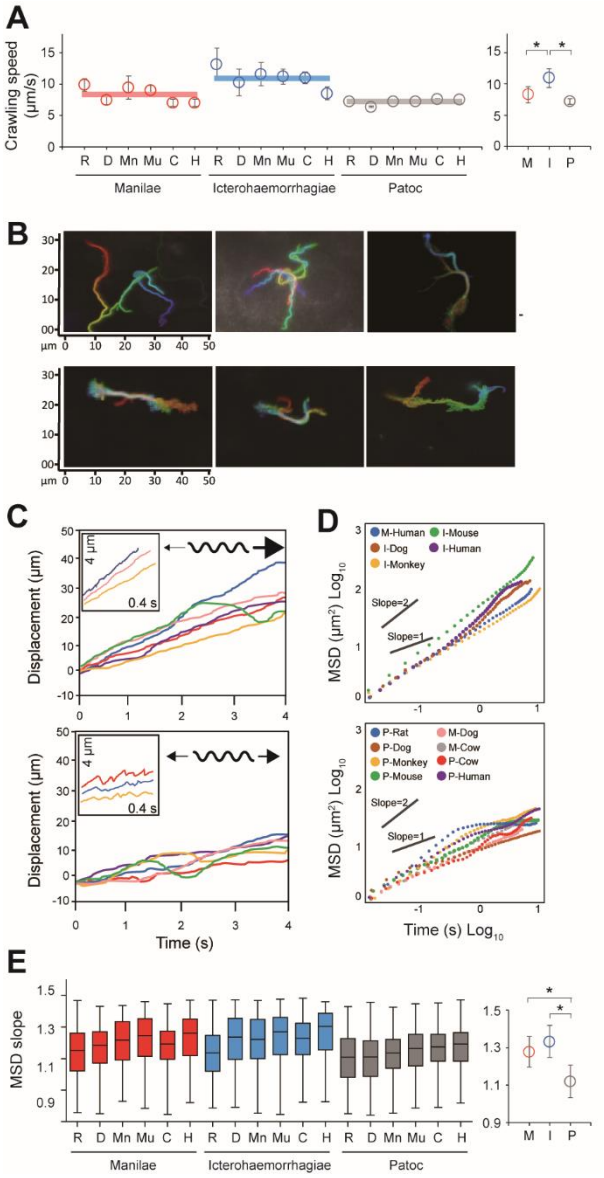

Fig. 3. Analysis of the crawling movement of *Leptospira* on kidney cell layers. (A) Average crawling speeds determined for each host-bacterium pair. More than 90 bacteria were measured for each pair. The averaged values calculated for each bacterial strain are shown by horizontal lines (left) and are plotted with the were (B) Examples of persistent crawling (upper panels) and diffusive crawling (lower panels) of *Leptospira* cells obtained by single-cell tracking in 10 s. Colors indicate time courses in the order of red orange yellow green blue, and indigo. (C) Example time courses of leptospires crawling on the kidney cell surfaces; inset, expanded view of cell displacements and schematics of motion patterns. The upper and lower panels show the long-distance migration

355 represented by directive crawling and the limited migration due to frequent reversal, respectively.
356 (D) Examples of MSD vs time plots, evaluating the directivity of individual leptospiral cell
357 movements: Plots with slopes ~ 2 indicate persistently directive crawling (upper), whereas those with
358 ~ 1 indicate a non-directional movement (lower), i.e., motion with high frequency of reversal
359 patterns and short net migration distance (refer to the schematic explanation of motion pattern in
360 insets of **C**). (E) MSD slopes determined for each host-bacterium pair. The boxes show the 25th (the
361 bottom line), 50th (middle), and 75th (top) percentiles, and the vertical bars show the minimum and
362 maximum values. The right panel show the strain-dependence of the medians. The statistical analysis
363 was performed by Mann-Whitney U test (* $P < 0.05$).
364
365

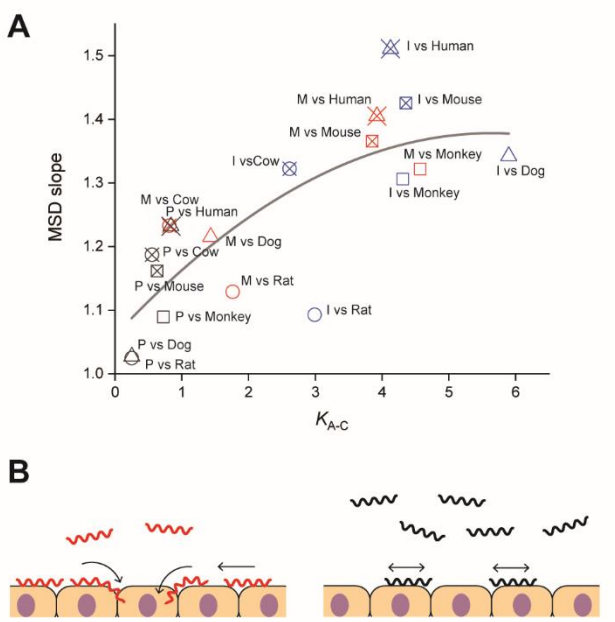

Fig. 4. Correlation of adhesion, motility and pathogenicity. (A) Relationship between $K_{A\text{-}C}$ and MSD slope (i.e., crawling persistency). The gray line is the result of quadratic curve fitting. The correlation coefficient is 0.77. See Fig. 2D for symbols. (B) A plausible model for crawling-dependent pathogenicity of *Leptospira*. In the cases that lead to severe symptoms (left), leptospiral cells were biased to the crawling state, and most of the crawling cells showed directional translation persistently over host tissue surfaces, increasing the invasion probability. For the asymptomatic or non-infectious cases, many leptospires remained in the swimming state and might be removed through body fluids or urination. Some fractions of the adhered leptospires were able to crawl, but their migration distances were limited due to frequent reversal.

Supplementary Materials

Title: Insight into motility-dependent pathogenicity of the zoonotic spirochete *Leptospira*

Authors: Jun Xu, Nobuo Koizumi, Shuichi Nakamura
Correspondence to: naka@bp.apph.tohoku.ac.jp

This file includes:

Other Supplementary Materials for this manuscript include the following:

393 **Table S1. Primer sequences used in this study**

Target	Primer sequence (5′→ 3′)	
	Forward	Reverse
rep-parB-parA (pGui1)	TCGACGCCGGCCAGCGGTTACTTCATAGCATCTTGGTTC	GCTGGAGCTCCACCGGCTCGACTCTTACGGTGTGTTAG
pNKLiG1 (pCjSpLe94 derivative)	CGGTGGAGCTCCAGCTTTG	GCTGGCCGGCGTCGAAAAGTAAGCACCTGTTATTGC
flgC promoter	TATCGATACCGTCGACCCGAGCTTCAAGGAAGATTTCCTA	ATGGAAACCTCCCTCATTTA
AcGFP	GAGGGAGGTTTCCATATGACCATGATTACGCCAAGC	TATCGATACCGTCGATCACTTGTACAGCTCATCCATG

394

395

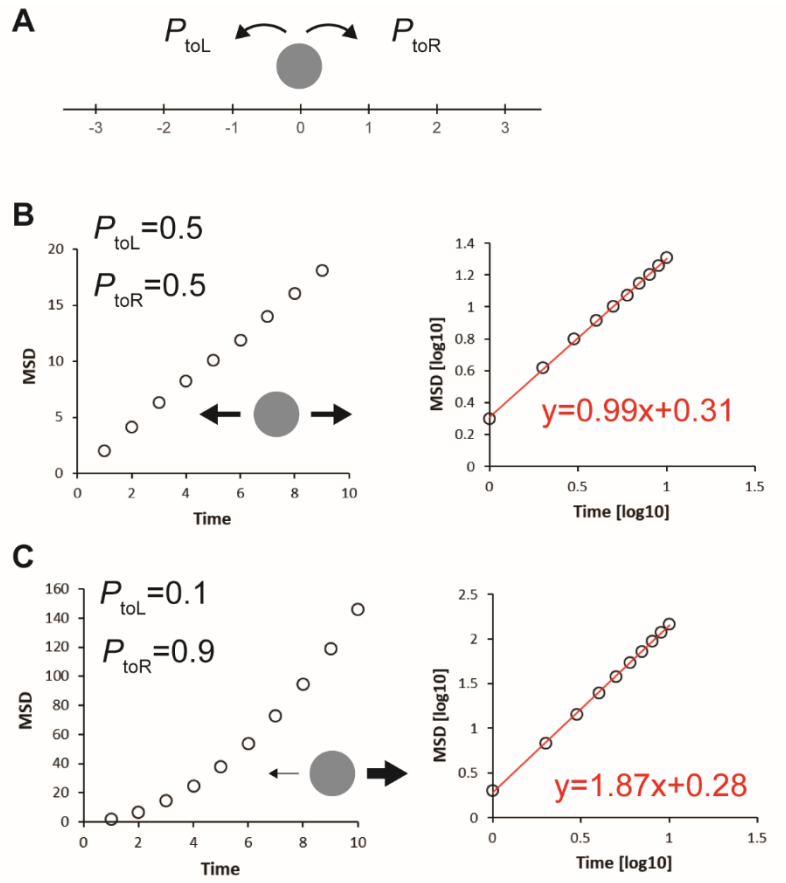

Fig. S1. Explanation of MSD plot. (A) To explain the difference in MSD vs time plot of "directed movement" (Figs. 3B-C upper) from that of "diffusive movement" (Figs. 3B-C lower), we performed a computer simulation by considering a particle stepping to the left (−1) or to the right (+1) with the probability of P_{toL} and P_{toR} (= 1−P_{toL}), respectively, in a time interval Δt. P_{toL} = 0.5 (P_{toR} = 0.5) and P_{toL} = 0.1 (P_{toR} = 0.9) were assumed for simulating simple diffusion and movement biased to the right, respectively, and the step direction was determined by a random number (*rnd*) from 0.0 to 1.0 generated in each event: If *rnd* < P_{toL}, the particle steps to the left (+1). The time course of the particle position was analyzed as shown in Methods. MSD vs time plots obtained by the simulation show that (B) simple diffusion and (C) directed movement give a linear line and a quadratic curve, respectively (left panels), therefore exhibiting linear lines with slopes of ∼1 and ∼2 in double-logarithmic plots (right panels). Red lines are regression lines fitted to data points obtained by simulation.

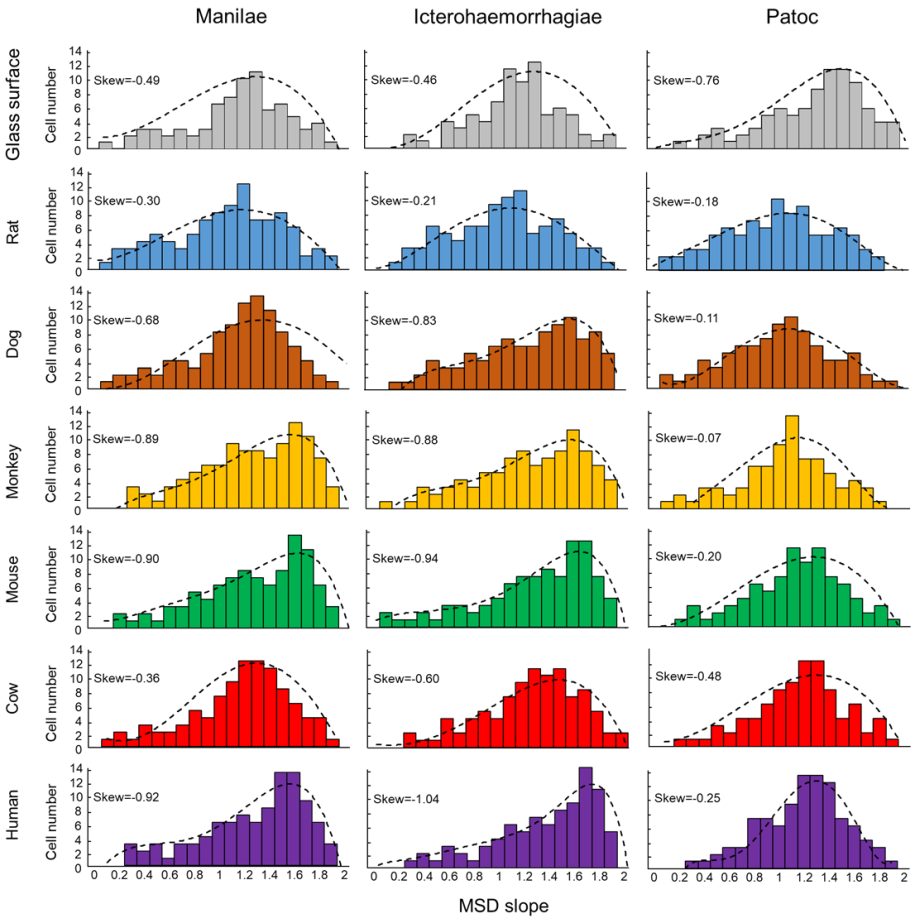

409

410 **Fig. S2. Histograms of the MSD slopes.** Dashed lines are the results of curve fitting.

411

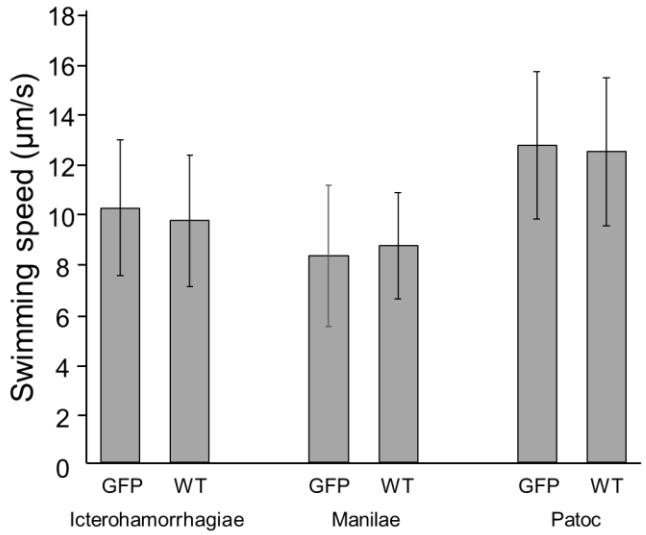

412

413 **Fig. S3. Effect of GFP expression on the *Leptospira* motility.** No significant different found
414 between the swimming speeds of GFP expressing strains and wild type strains in each serovar.

415

416